

## Energies of $\pi$ -Mesonic X-Rays\*

MARTIN STEARNS AND MARY BETH STEARNS  
Carnegie Institute of Technology, Pittsburgh, Pennsylvania

(Received May 16, 1956)

The energies of the  $2p \rightarrow 1s$  x-rays from the  $\pi$ -mesonic atoms Li through F have been measured to  $\frac{1}{2}\%$  or better. All the measured energies were lower than those calculated from the Klein-Gordon equation assuming a point-charge Coulomb field and corrected for finite size effects and vacuum polarization. (These are the only non-negligible electromagnetic corrections.) This indicates that the net nuclear interaction between a meson in the  $1s$  orbit and a nucleus is repulsive. The energy shifts varied in a fluctuating manner from 3.4% for Li to 11.7% for O and 11.4% for F. If we assume that the shift arises from a scattering type potential, and further, that the effects of the individual nucleons are simply additive, then values for the  $s$ -wave scattering lengths  $a_1$  and  $a_3$  can be obtained by a least squares fit to the data. The values of  $a_1$  and  $a_3$  obtained in this manner are  $a_1 = 0.14\lambda_\pi$  and  $a_3 = -0.10\lambda_\pi$ . The  $K_\alpha$  energies of the isotopes  $B^{10}$  and  $B^{11}$  were measured separately, thus giving a direct determination of  $a_3$  under the previous assumptions. This value for  $a_3$  is  $(-0.12 \pm 0.02)\lambda_\pi$ .

The energies of  $\pi$ - $L_\alpha$  x-rays for Si, Cl, K, and Ca were also measured but with less accuracy. They were all found to agree with the calculated energy values to within 1% or better.

A rough measure of the width of the  $B^{10}$   $K_\alpha$  line was also obtained.

### I. INTRODUCTION

MESONIC spectroscopy has in recent years become an increasingly important technique in nuclear investigations.<sup>1-3</sup> This work can be broadly divided into two groups. The first group consists of studies of meson-nucleus interactions which are essentially electromagnetic in character; they would scarcely be altered if the meson were simply an electron of appropriate mass, spin, and magnetic moment. Much of this work is a logical extension of the more familiar studies in electron spectroscopy—particularly the investigation of nuclear effects in electron hyperfine structure. In this first group are effects due to the structure and finite extent of the nucleus, nuclear polarization, nuclear spins and quadrupole moments, vacuum polarization, etc. Most of these have been calculated in considerable detail and are discussed in the following section. Nearly all  $\mu$ -meson work falls into this group.<sup>4</sup> Also  $\pi$ -meson experiments giving information on the Auger effect<sup>5,6</sup> and the  $\pi$ -meson mass<sup>7</sup> properly belong in this category.

The second group is comprised of studies of the specific (nonelectromagnetic) meson-nuclear interaction. This interaction, weak in the case of  $\mu$  mesons, is of great importance for  $\pi$  mesons. The radiative yields<sup>5,6</sup>

and energies<sup>8</sup> of pi-mesonic x-rays fall into this category. This paper is a report on recent measurements of the  $1s$  and  $2p$  energy levels of  $\pi$ -mesonic atoms. The radiative yields of the  $K$ ,  $L$ , and  $M$  series will be reported in subsequent papers.

### II. CALCULATIONS OF ENERGY LEVELS

Because of the strong pion-nuclear interaction,  $\pi$  mesons are absorbed directly from higher energy levels, the absorption increasing rapidly with increasing atomic number. Absorption from the  $2p$  level is practically complete at Na ( $Z=11$ ). For this reason measurements of the  $2p \rightarrow 1s$  pi-mesonic x-rays are necessarily limited to light elements. This simplifies the calculation of energies. Neglecting the specific pion-nuclear interaction, we can treat the mesonic atom, in the case of light elements, as a hydrogen-like atom in zeroth approximation. The perturbations mentioned in Sec. I, being small for small  $Z$ , can be calculated to first order in a straightforward manner. The corrected calculated energy levels are then compared with the experimental values. Any deviation between the calculated and measured values we attribute to the specific pion-nuclear interaction, neglected in the calculation.

In zeroth approximation the energy levels of the  $\pi$  meson, with spin 0, are adequately described by the Klein-Gordon equation

$$E_{n,l} = -\frac{Z^2\alpha^2\mu}{2n^2} \left[ 1 + \frac{Z^2\alpha^2}{n^2} \left( \frac{n}{l+\frac{1}{2}} - \frac{3}{4} \right) + \dots \right], \quad (1)$$

where  $\mu$  is the reduced mass,  $\alpha$  the fine structure constant, and  $n$  and  $l$  the principal and orbital quantum numbers respectively. We have used for the free  $\pi$ -meson mass the value<sup>9</sup>  $m_\pi = 272.8m_e$ .

<sup>8</sup> Stearns, Stearns, DeBenedetti, and Leipuner, Phys. Rev. **96**, 804 (1954); Phys. Rev. **97**, 240 (1955).

<sup>9</sup> The most recent value is  $(272.8 \pm 0.3)m_e$ . Barkas, Birnbaum, and Smith, Phys. Rev. **101**, 778 (1956).

\* Work supported by the U. S. Atomic Energy Commission.

<sup>1</sup> J. A. Wheeler, Revs. Modern Phys. **21**, 133 (1949); Phys. Rev. **92**, 812 (1953).

<sup>2</sup> L. N. Cooper and E. M. Henley, Phys. Rev. **92**, 80 (1953).

<sup>3</sup> V. L. Fitch and J. Rainwater, Phys. Rev. **92**, 789 (1953).

<sup>4</sup> An important exception is the measurement of the  $\mu$ -meson lifetime in condensed materials, first observed by Conversi, Pancini, and Piccioni and subsequently studied by Keuffel, Ticho, Lederman, and others.

A report of the  $K$  and  $L$  radiative yields from  $\mu$ -mesonic atoms is in preparation.

<sup>5</sup> Stearns, DeBenedetti, Stearns, and Leipuner, Phys. Rev. **93**, 1123 (1954).

<sup>6</sup> Camac, Halbert, and Platt, Phys. Rev. **99**, 905 (1955); Camac, McGuire, Platt, and Schulte, Phys. Rev. **99**, 897 (1955).

<sup>7</sup> Stearns, Stearns, DeBenedetti, and Leipuner, Phys. Rev. **95**, 1353 (1954).

Electromagnetic corrections which must be considered are the following.

### A. Finite Extent of the Nucleus

This Coulomb correction is negligible for all but  $s$  states. Its effect is to raise the  $1s$  level. It is extremely large in the case of heavy nuclei as shown by the work of Fitch and Rainwater.<sup>3</sup> For light nuclei, however, it can be treated as a perturbation on the Schrödinger equation for a point charge. The first-order correction for  $s$  states (assuming a uniform nuclear charge distribution) is given by<sup>2</sup>

$$\Delta E_{n,s} = -\frac{4}{5} \frac{1}{n^3} \left( \frac{ZR}{r_B} \right)^2 E_Z, \quad (2)$$

where  $R$  is the nuclear radius, taken to be  $1.2 \times 10^{-13} A^{\frac{1}{3}}$ ,  $r_B$  is the  $\pi$  meson Bohr orbit,  $\hbar^2/\mu e^2$ , and  $E_Z$  is the Rydberg,  $Z^2 e^2/2r_B$ . For the  $2p$  state<sup>10</sup>

$$\Delta E_{2p} = E_Z \left[ 0.0016 \left( \frac{ZR}{r_B} \right)^4 - 0.0011 \left( \frac{ZR}{r_B} \right)^5 + \dots \right], \quad (3)$$

which is negligible, even for  $Z \sim 20$ .

Corrections to the  $1s$  level are given in Table II, column 3. The percentage corrections to the  $2p \rightarrow 1s$  energies vary from about 0.1% in Li to 2.5% in F.

### B. Vacuum Polarization

This is the only significant radiative correction to the energy levels of mesonic atoms. Its effect is to lower all levels, the  $1s$  more than the  $2p$ , etc. (The self-energy correction, which is predominant in the shift of  $s$  levels in normal electronic atoms, arises from the coupling of the orbital particle to the radiation field. Since, in first-order approximation, this coupling is inversely proportional to the square of the mass of the orbital particle, its effect on mesons is very small. The vacuum polarization, on the other hand, modifies the electrostatic potential in a manner independent of mass.)

The vacuum polarization effect has been calculated to first order ( $\alpha Z$ ) by Mickelwait and Corben<sup>11</sup> and their results are given in Table II, column 4. (Higher order corrections have been examined by Wichmann and Kroll<sup>12</sup> and are completely negligible for the present work.) The net vacuum polarization correction to the  $2p \rightarrow 1s$  transition is about 0.4% for Li and rises to 0.7% in F.

### C. Hyperfine Structure (Nuclear Spin-Meson Orbit Interaction)

This arises from the interaction between the magnetic moment of the nucleus and the magnetic field produced

at the nucleus by the meson current. (Since the  $\pi$  meson has zero spin there is no spin-spin interaction.) The energy shift is given, in first approximation, by

$$\Delta E = -\mathbf{u} \cdot \mathbf{H} = -\left( \frac{e\hbar}{2Mc} \mathbf{I} \right) \cdot \left( \frac{e\hbar}{\mu c} \left\langle \frac{1}{r^3} \right\rangle \mathbf{l} \right), \quad (4)$$

where  $g$  is the nuclear  $g$  factor,  $\mathbf{I}$  the nuclear vector spin, and  $\mathbf{l}$  is the meson orbital angular momentum. For  $l \neq 0$ , Eq. (6) becomes

$$\Delta E_{n,l} \simeq -\frac{gZ\alpha^2 [F(F+1) - I(I+1) - l(l+1)]}{13.5 n^3 l(l+\frac{1}{2})(l+1)} E_Z, \quad (5)$$

where  $\mathbf{F}$  is the total angular momentum,  $\mathbf{I} + \mathbf{l}$ .

Since the interaction goes as  $\langle 1/r^3 \rangle$ , states with the smallest  $n$  and  $l$  will be most affected. An estimate of the shift of the  $2p$  level can be made with some reasonable values of the parameters. Let  $g=7$ ,  $Z=10$ ,  $n=2$  and set  $F$ ,  $I$ , and  $l$  each equal to unity. Then Eq. (7) gives  $\Delta E_{2p} = 2.3 \times 10^{-5} E_Z$  (about 8 ev), which is negligible.

For  $l=0$ , Eq. (7) is indeterminate. However, a reasonable estimate of the shift of the  $1s$  level can be obtained by arbitrarily canceling the zero quantities before setting  $l=0$ . For  $g=7$ ,  $Z=10$  this gives  $\Delta E_{1s} \sim 2 \times 10^{-4} E_Z$ . Even though this is ten times larger than the  $2p$  shift, it is still negligible for the present work.

### D. Nuclear Quadrupole Moment

The effect of the nuclear quadrupole moment on meson energy levels has been calculated by Wheeler.<sup>1</sup> Although he is particularly interested in the level splitting of the  $2p_{\frac{1}{2}}$  state of the  $\mu$  meson, we can use his expression to get an estimate of the maximum energy shift of the  $\pi$ -meson state. The width of the pattern produced by the quadrupole interaction, as given by Wheeler, is

$$\Delta E \simeq 1 \text{ Mev} (Q/10^{-24} \text{ cm}^2) (Z/237)^3 f_Q, \quad (6)$$

where  $Q$  is the quadrupole moment and  $f_Q$  is a form factor of the order of unity. Since in the present work  $Z < 20$  and  $Q \ll 1$ , the quadrupole interaction is small.

### E. Nuclear Polarization

It has been assumed in all the effects discussed earlier that the meson interacts with the *static* field of the nucleus, i.e., the nucleus is unaffected by the meson. This neglects the coupling between the energy states of the nucleus and those of the meson. (The meson excites the nucleus and changes its energy.) In nuclei with large deformations, and thus low-lying excited states, this coupling can be significant. In the lighter elements, however, the effect is small. Nuclear polarization has been studied by Cooper and Henley,<sup>2</sup>

<sup>10</sup> S. W. Flügge, from lecture notes on meson problems given at Carnegie Institute of Technology (unpublished).

<sup>11</sup> A. B. Mickelwait and H. C. Corben, Phys. Rev. **96**, 1145 (1954).

<sup>12</sup> E. H. Wichmann and N. M. Kroll, Phys. Rev. **101**, 843 (1956).

Wilets,<sup>13</sup> Jacobsohn,<sup>14</sup> and Lakin and Kohn.<sup>15</sup> Lakin<sup>16</sup> has made estimates of this effect for some of the light elements we use and in all cases has found them negligible;  $\Delta E/E < 10^{-4}$ .

### F. External Electron Screening

The effect of the electron cloud external to the meson orbit is to modify the Coulomb potential in the familiar way,<sup>17</sup>

$$V = -\frac{Ze^2}{r} \Psi\left(\frac{r}{b}\right), \quad (7)$$

where  $\Psi(r/b)$  is the screening factor. ( $b$  is a length with dimensions of the order of the radius of the electron Bohr orbit.) For  $r$  small,  $\Psi(r/b)$  can be approximated sufficiently accurately by expanding the Fermi-Thomas screening factor. This gives

$$\Psi(r/b) \simeq 1 - 1.589r/b + \dots \quad (8)$$

The perturbing potential is then

$$\Delta V = V - (Ze^2/r) = 1.589Ze^2/b = \text{constant}. \quad (9)$$

Since the perturbation is a constant, the effect to first order is to shift all levels the same amount. Therefore the transition energies between states will be unmodified.

### G. Internal Electron Screening

The effect of internal screening by the fraction of the electron cloud inside the meson orbit can be estimated as follows: The potential,  $\phi$ , due to the electronic charge density,  $\rho$ , is given by Poisson's equation. A spherical charge distribution gives

$$\phi = \text{constant} - \frac{2}{3}\pi\rho r^2. \quad (10)$$

The constant term can be neglected since its effect is to shift all the meson levels the same amount.  $\rho$  can be approximated by

$$\rho \simeq -e \sum_i |\psi_i(0)|^2, \quad (11)$$

where the summation is over all the  $s$  electrons. Combining Eqs. (10) and (11), we get the energy shift to first order,

$$\Delta E = \langle -e\phi \rangle = \frac{2}{3}\pi e^2 \sum_i |\psi_i(0)|^2 \langle r^2 \rangle. \quad (12)$$

This expression has been evaluated for the  $4f \rightarrow 3d$  transition in phosphorous and gives a net shift of about

<sup>13</sup> L. Wilets, Kgl. Danske Videnskab. Selskab, Mat-fys. Medd. 29, No. 3 (1954).

<sup>14</sup> B. A. Jacobsohn, Phys. Rev. 96, 1637 (1954).

<sup>15</sup> W. Lakin, thesis, Carnegie Institute of Technology (unpublished).

<sup>16</sup> W. Lakin (private communication). Also W. Lakin and W. Kohn, Phys. Rev. 94, 787(A) (1954).

<sup>17</sup> See, for example, L. I. Schiff, *Quantum Mechanics* (McGraw-Hill Book Company, Inc., New York, 1949), Chap. XI.

1 ev, or  $\Delta E/E = 3 \times 10^{-5}$ . This is negligible. The shifts for  $K$  and  $L$  lines will be even less since, as can be seen from Eq. (12), the shifts increase as the average square of the meson-nucleus distance and therefore approximately as  $n^4$ .

### III. EXPERIMENTAL PROCEDURE

The experimental arrangement is shown schematically in Fig. 1. Pi-mesons of about 110-Mev energy were slowed down in the copper plus beryllium absorber and came to rest in the target of the element investigated. The number of stopped mesons was indicated by the coincidence of counters 1, 2, and 3 in anti-coincidence with counter 4 ( $\sim 2 \times 10^{-8}$  sec). The mesonic x-ray was detected in the NaI crystal. To trigger the pulse-height selector (p.h.s.), the combination  $(1+2+3-4)$  was required to coincide (within  $\sim 5 \times 10^{-8}$  sec) with a clipped pulse from the last dynode of the NaI photomultiplier. The thicknesses of counters 3, 4, and the NaI crystal were varied depending on the energy of the line under investigation and on the target material used. Details of the experimental setup will be discussed more fully in a future article.

The energies of the  $2p \rightarrow 1s$  ( $K_\alpha$ ) lines investigated varied from about 20 kev to 200 kev. They were measured in two different ways. The first, and in most cases the least accurate method, was that of the critical absorption technique familiar from x-ray work. The absorber (filter) was inserted between counter No. 4 and the NaI crystal. If the energy of the line investigated was greater than that of the  $K$  edge of the filter the line was strongly absorbed; if less than the  $K$  edge it was mostly transmitted. The transmission of a given  $2p \rightarrow 1s$  line was measured as a function of the  $Z$  of the filter.

The second method was to determine the energy of the  $K_\alpha$  line by a measurement of pulse height. The experimental procedure was to bracket each  $K_\alpha$  line under investigation with two calibration lines of similar energy and these were run alternately several times. The stability of the apparatus allowed a determination of the  $K_\alpha$  energy to 1% or better for the elements investigated, Li through F.

Several checks were made to insure that there was no energy degradation due to Compton scattering or  $\mu$ -meson contamination. Broad plane radioactive sources were prepared with energies varying from 60 kev to

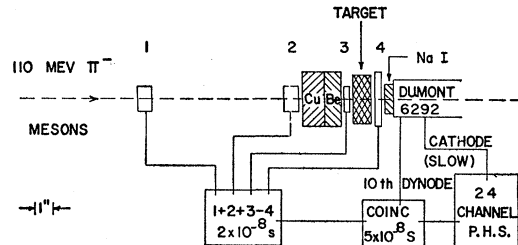


FIG. 1. Experimental arrangement. (Cathode should read anode.)

250 kev. Their spectra were first measured with the NaI detector without any intervening material. They were then measured with counter No. 4 placed before the NaI crystal and the sources surrounded by various target materials. A slight broadening on the low-energy side of the spectra was observed; however, it was never sufficient to cause any discernible shift in peak position. (Additional tests for energy degradation made with the Be  $K_\alpha$  line are discussed in the following section on Be.) There was no evidence of  $\mu$ -meson contamination. Long runs on  $\pi$ -meson lines for which the yield is nearly zero gave no sign of a (lower energy)  $\mu$ -meson line.

#### IV. EXPERIMENTAL RESULTS

##### A. Energies from Critical Absorption Measurements

To verify that this technique could be usefully applied to mesonic x-rays, we tested it with lines of known energy:  $\pi$ - $L_\alpha$ (N,O,F,Mg,Al);  $\pi$ - $M_\alpha$ (P,Al,K);  $\mu$ - $K_\alpha$ (Be), etc. In all instances the measurements gave correct and sensible results. The transmitted intensity always showed an abrupt discontinuity between two adjacent absorbers ( $\Delta Z = 1$ ) whenever the line energy lay between the two corresponding  $K$  edges. Use was made of this feature to determine the  $\pi$ -meson mass.<sup>7</sup> This will be discussed further in a subsequent article.

A description of the application of the critical absorber technique to the individual  $K_\alpha$  lines follows. Table I is a summary of the results.

**Lithium.**—The Li target had the normal isotopic mixture (92%  $\text{Li}^7$  and 8%  $\text{Li}^6$ ). The critical absorbers were foils, varying from Rh ( $Z=45$ ) to Cd ( $Z=48$ ). Their thickness was such that the transmission was 50% for an x-ray whose energy was just below that of the  $K$  edge of the foil. Figure 2 shows curves of transmitted intensity and peak positions obtained with the various foils. It is apparent that there is a discontinuity in transmission between the Pd and Rh foils, the Rh foil absorbing a much larger fraction of the incident  $\text{Li}(K_\alpha)$  line. Since "poor geometry" was used in these measurements, much of the fluorescent radiation from the foil was detected by the NaI crystal. Therefore the intensity transmitted through a filter whose  $K$  edge was excited by the mesonic x-ray line should be expected to be roughly a factor two to four less (depending on the fluorescent yield and filter thickness) than the intensity

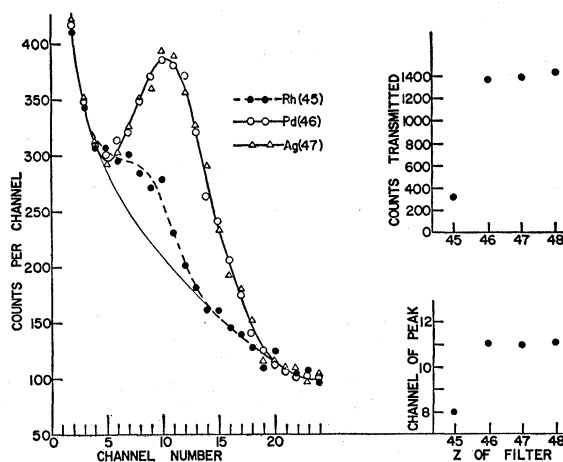


FIG. 2. Transmission curves for  $\text{Li}(K_\alpha)$  x-rays through critical absorbers placed between the target and the NaI detector. The  $K$  electrons of the Pd and Ag filters are not excited by the  $\text{Li}(K_\alpha)$  x-rays, whereas the Rh filter strongly absorbs them. The peak observed with the Rh filter is due to fluorescent radiation; note that it has moved to a lower channel.

transmitted through a filter whose  $K$  edge was not excited by the incident x-rays. The peak position, moreover, should be shifted downward since the fluorescent radiation has lower energy. As can be seen in Fig. 2, plots of "counts transmitted *vs*  $Z$ " and "peak position *vs*  $Z$ " indicate both of these features very clearly.

The  $\text{Li}(K_\alpha)$  line is observed to be between the  $K$  edges of Rh and Pd. Its energy, therefore, is within the limits  $23.22 \text{ kev} < E < 24.35 \text{ kev}$ .<sup>18</sup>

**Beryllium-9.**—(100%) The filters were thin-walled Lucite cells, 1 cm thick, containing an aqueous solution of a salt of the absorbing element (usually a nitrate). The concentration of each cell was adjusted to give 75% transmission for x-rays whose energy was just below the  $K$  edge. (This corresponds to a factor of four in the transmission of x-rays with energies just below and above the  $K$  edge.) Figure 3 shows some typical results of "counts transmitted" and "peak positions" obtained for Be. We were very fortunate in the case of Be since the Pr  $K$  edge splits the  $\text{Be}(K_\alpha)$  line. This is clearly indicated in Fig. 3 where for  $Z=59$  (Pr) the yield and peak position curves are about midway between their extreme values. (These features were consistently observed in six independent runs.) This behavior indicates that the  $\text{Be}(K_\alpha)$  energy is very close to 41.98 kev.

Because the  $\text{Be}(K_\alpha)$  energy line straddles the Pr  $K$  edge it should provide a sensitive test as to whether or not there is much energy degradation in the targets. For this purpose we investigated two different Be targets, one  $\frac{1}{2}$  in. thick and the other 1 in. thick. The results obtained were not discernibly different for the

TABLE I.  $K_\alpha$  energies obtained from critical absorber measurements.

Element	Calculated energy (kev)	Measured energy (kev)
$^3\text{Li}$	24.61	$23.22 < E < 24.35$
$^4\text{Be}^9$	43.95	close to 41.98
$^5\text{B}^{10}$	68.76	close to 65.2
$^6\text{B}^{11}$	68.83	$61.31 < E < 65.32$
$^6\text{C}^{12}$	99.10	$90.53 < E$

<sup>18</sup> We are very grateful to J. W. M. DuMond and R. L. Shacklett for measuring the  $K$ -edge profiles of many of the filters used in our experiments.

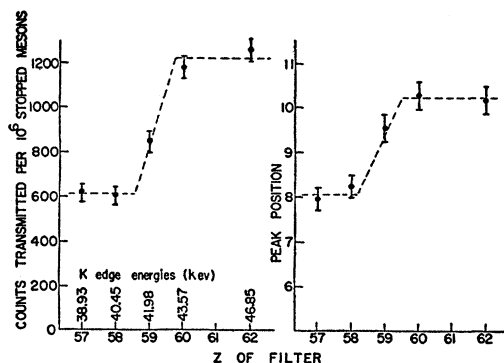


FIG. 3. Plots of the counts transmitted and peak position of  $\text{Be}(K_\alpha)$  x-rays vs  $Z$  of the filter. The  $^{59}\text{Pr}$  absorber removes about one-half of the x-rays indicating that the  $\text{Be}(K_\alpha)$  x-rays have an energy very close to 41.98 kev.

two targets, again giving evidence that energy degradation in the targets was negligible.

**Boron-10 and Boron-11.**—The boron used in the initial experiments was contaminated with Mg and led to anomalous results. These disappeared after we acquired purer boron.<sup>19</sup> Two different sets of filters were used. The first set was composed of filters similar to those described in the Be measurements. Unfortunately, the elements with  $K$  edges below the  $\text{B}(K_\alpha)$  energy are in the rare earth region and some were unobtainable. Both  $\text{B}^{10}$  and  $\text{B}^{11}$  gave discontinuities in the transmission and peak position curves between  $^{70}\text{Yb}$ <sup>20</sup> and  $^{72}\text{Hf}$ , indicating that the energies of both isotopes lie between the limits  $61.31 \text{ kev} < E < 65.32 \text{ kev}$ . ( $^{71}\text{Lu}$  could not be acquired.)

However, because of the sizeable linear thickness of the cells (with consequent poor solid angle), the transmission discontinuities in this case were not as large or clean as we desired. Moreover, pulse-height measurements of  $\text{B}^{10}$ , to be described in the next section, indicated that the  $\text{B}^{10}(K_\alpha)$  energy was very close to the Hf  $K$  edge. For these reasons we ran another series of transmission experiments with foils of Hf,<sup>21</sup> Ta, and W. Each of these were of such thickness as to transmit about 56% of incident radiation if the energy were just below the  $K$  edge, about 3% if just above. In the latter case the resultant fluorescent radiation would increase the apparent transmission to about 18%. With these foils discontinuities, or partial discontinuities, should show up very clearly because of the close geometry and large effective foil thickness. As can be seen in Fig. 4 the  $\text{B}^{10}$  x-rays are indeed partially reduced by the Hf foil; only 75% as many x-rays are transmitted as by the Ta and W foils. [The dashed curve indicates the transmission expected through a filter whose  $K$  edge is below the  $\text{B}^{10}(K_\alpha)$  energy.] From this

information we conclude that the energy of the Hf  $K$  edge lies within the natural width of the  $\text{B}^{10}(K_\alpha)$  line. Furthermore, by using the  $\text{B}^{10}$  energy obtained from the pulse-height measurements ( $65.2 \pm 0.2 \text{ kev}$ ), and assuming a Gaussian shape for the  $2p \rightarrow 1s$  line, we can get a rough measure of the half-width of the  $\text{B}^{10} 1s$  level. The value obtained is  $1.1 \pm 1.4 \text{ kev}$ . This is of the same order of magnitude as the half-width given by Brueckner,<sup>22</sup> about 1.1 kev.

**Carbon.**—Naturally occurring carbon was used (98.9%  $\text{C}^{12}$ ). The filters were aqueous solutions prepared in the same manner as the Be filters. We were able to obtain only elements whose  $K$  edges were below the  $\text{C}(K_\alpha)$  energy.  $^{80}\text{Hg}$ ,  $^{82}\text{Pb}$ , and  $^{83}\text{Bi}$  filters gave the same transmission, indicating that the energy of the  $\text{C}(K_\alpha)$  line is greater than 90.53 kev.

## B. Energies from Pulse-Height Measurements

As noted earlier, the experimental procedure was to bracket the unknown  $K_\alpha$  line with two calibration lines whose energies were well known and close to that of the  $K_\alpha$ . A  $K_\alpha$  run was always preceded and followed by runs of both calibration lines. The over-all stability of the electronic apparatus was such that drifts during such a sequence of runs were 1% or less.

In order to insure stability and reproducibility we found it necessary to run at constant beam level and to avoid changes in amplifier and attenuator settings during a sequence of runs. One of the principal sources of drifts in previous measurements was the change in pulse height of the NaI detector due to changes in

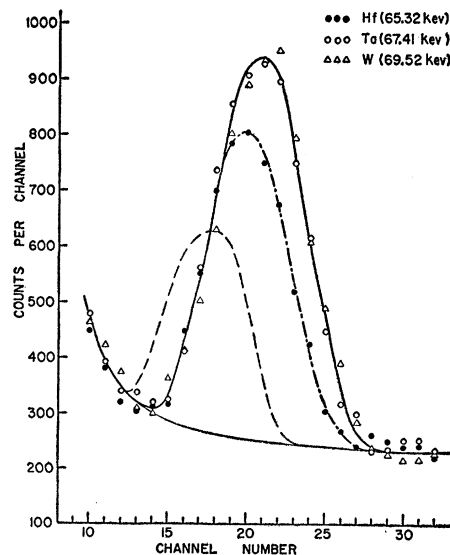


FIG. 4. Transmission curves for  $\text{B}^{10}$  with Hf, Ta, and W filters. The Hf absorbs about 25% more x-rays than the Ta and W. The dashed curve shows the expected transmission for a filter whose  $K$  edge is slightly lower in energy than the  $\text{B}^{10}(K_\alpha)$  line. This indicates that the Hf  $K$  edge falls within the natural width of the  $\text{B}^{10}(K_\alpha)$  line.

<sup>19</sup> We thank the Oak Ridge National Laboratory for a loan of enriched  $\text{B}^{10}$ .

<sup>20</sup> We are grateful to F. H. Spedding for a loan of Yb.

<sup>21</sup> We thank the Westinghouse Laboratories for a loan of the Hf foil.

<sup>22</sup> K. A. Brueckner, Phys. Rev. 98, 769 (1955).

TABLE II. Calculated  $K_\alpha$  energies and experimental values from pulse-height measurements.

Transition	Energy from Klein-Gordon equation <sup>a</sup>	Finite size correction (kev)	Vac. polar. correction (kev)	Calculated energy (kev)	Measured energy <sup>b</sup> (kev)	Energy shift (kev)	Percent shift
Li( $K_\alpha$ )	24.546	-0.033	0.096	24.61	$23.77 \pm 0.12$	0.84	$3.4 \pm 0.5$
N( $L_\alpha$ )	25.004		0.064	25.07			
O( $L_\alpha$ )	32.708		0.094	32.80			
F( $L_\alpha$ )	41.464	-0.123	0.136	41.60	$42.09 \pm 0.10$	1.86	$4.2 \pm 0.25$
Be( $K_\alpha$ )	43.869		0.202	43.95			
S( $M_\alpha$ )	46.022		0.126	46.15			
Na( $L_\alpha$ )	62.056	-0.324	0.230	62.29	$65.2 \pm 0.2$	3.5 <sub>4</sub>	$5.15 \pm 0.3$
B <sup>10</sup> ( $K_\alpha$ )	68.708		0.376	68.76			
B <sup>11</sup> ( $K_\alpha$ )	68.802		0.376	68.83			
Mg( $L_\alpha$ )	73.894	-0.347	0.288	74.18	$63.5 \pm 0.2$	5.35 <sup>c</sup>	$7.8 \pm 0.3$
Al( $L_\alpha$ )	86.801	-0.765	0.365	87.17	$92.6 \pm 0.4$	6.5	$6.5 \pm 0.4$
C( $K_\alpha$ )	99.284		0.576	99.10			
Si( $L_\alpha$ )	100.72		0.430	101.15			
P( $L_\alpha$ )	115.73	-1.57	0.53	116.26	$126.0 \pm 0.3$	8.8	$6.55 \pm 0.2$
N( $K_\alpha$ )	135.52		0.84	134.79			
S( $L_\alpha$ )	131.74		0.63	132.37			
Cl( $L_\alpha$ )	148.84	-2.93	0.74	149.58	$155.2 \pm 0.8$	20.5	$11.7 \pm 0.5$
O( $K_\alpha$ )	177.46		1.20	175.73			
Zn( $M$ )				$159.45 \pm 0.25$			
K( $L_\alpha$ )	186.16	-5.28	0.97	187.13	$196.3 \pm 1.0$	25.3	$11.4 \pm 0.5$
F( $K_\alpha$ )	225.25		1.60	221.57			
Ca( $L_\alpha$ )	206.38		1.10	207.48			

<sup>a</sup>  $m_\pi = 271.8 m_e$ .<sup>b</sup> The errors quoted are rms values; see text for discussion of possible systematic errors.<sup>c</sup>  $E_{B^{10}} - E_{B^{11}} = 1.8 \pm 0.3$  kev; percent difference in energy shift =  $(2.65 \pm 0.5)\%$ .

beam level. (This effect has been observed by others when using DuMont 6292 photomultiplier tubes.) Because of these limitations we used only  $\pi$ —( $L_\alpha$  or  $M_\alpha$ ) lines for calibration. Natural sources or  $\mu$  lines, which we used in some preliminary measurements, altered the beam level and were, therefore, unreliable. The use of  $\pi$  lines for calibration has the additional advantage of reducing systematic errors.

Another modification of our earlier preliminary setup was the use of thin  $\frac{1}{8}$ -in. plastic scintillators for counters No. 3 and No. 4 instead of the earlier thicker stilbene crystals. This change not only resulted in an increased counting rate since it moved the target closer to the detector, but, in addition, it decreased the carbon contamination due to mesons stopping in counter No. 3. It was essential to reduce this carbon contamination in order to get reliable measurements of the N and O energies.

The mesonic x-rays were measured with NaI crystals,  $\frac{1}{2}$  in. in diameter, and of a thickness depending on the energy. For the Li( $K_\alpha$ ) and Be( $K_\alpha$ ) measurements the crystal was  $\frac{1}{16}$  in. thick and had a 5-mil aluminum window. The efficiency was 70–85% for x-rays of 20–80 kev. (This considers attenuation in the target, counter No. 4, and the aluminum window, but does not include the solid-angle factor.) A  $\frac{1}{2}$ -in. thick NaI crystal was used to measure x-rays from the elements B through F (60–200 kev). The efficiency was about 80–85% for x-rays between 50 and 150 kev—again including only attenuation factors. It was felt that the efficiency above

150 kev was known with sufficient accuracy to adequately correct the spectra at higher energies. Efficiency and background corrections were made only for  $K$  lines and for  $L$  lines of small  $Z$ . (For the  $M$  lines used and for  $L$  lines of  $Z > 11$ , the backgrounds are quite flat and the ratio of peak to background large; thus the peak position is insensitive to whether or not the background is subtracted.)

A description of the pulse-height measurements of the individual  $K_\alpha$  lines follows. A summary of the results, as well as the calculated energies, is given in Table II. The percent energy shift listed in the table is defined by  $[(E_{\text{calc}} - E_{\text{meas}})/E_{\text{calc}}] \times 100$ .

*Lithium.*—The Li target had the normal isotopic mixture (92% Li<sup>7</sup> and 8% Li<sup>6</sup>). N( $L_\alpha$ ) and O( $L_\alpha$ ) lines were used for calibration. The resolution of the NaI detector ( $\sim 40\%$ ) is so poor in this energy region that it is difficult to select the peak position and impossible to separate out higher transitions. This limited instrumental resolution can be turned to advantage, however, since it makes the shape of the curves—in particular the leading edge, where there is no contamination from higher transitions—the same for all three lines. It was observed, in fact, that when background was subtracted and the peaks normalized to equal height, the leading edges were indeed parallel and one could measure their displacements from each other quite accurately. In view of this we have used the midpoint of the leading edge of the curves for the energy determinations. As will be seen, this method gives very reliable results.

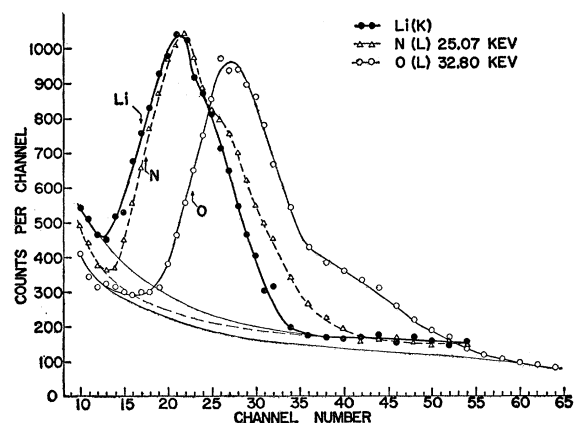


FIG. 5. Curves of the Li(K) x-rays and its calibration lines before background subtractions were made. (Each curve is a composite of several runs taken with the p.h.s. centered at different energies.) The bumps on the high energy side, especially noticeable in the L lines, are due to the higher transitions.

Figure 5 shows a typical run of Li and its calibration lines before backgrounds were subtracted. Because the calibration lines have essentially the same energy and shape as the Li( $K_\alpha$ ) spectrum any errors in the background subtraction and inefficiency of detection tend to cancel out. The energy obtained from the average of four runs similar to that shown in Fig. 4 is  $(23.77 \pm 0.12)$  kev. The error quoted is the rms error of the several runs. This energy is 0.84 kev less than the calculated energy, giving an energy shift of  $(3.4 \pm 0.5)\%$ .

The energy obtained here is in excellent agreement with a recent value  $(23.8 \pm 0.1)$  kev) measured by West and Bradley,<sup>23</sup> who used a proportional counter as the x-ray detector.

*Beryllium-9 (100%).*—The calibration lines were F( $L_\alpha$ ) and S( $M_\alpha$ ). Figure 6 shows a typical run with

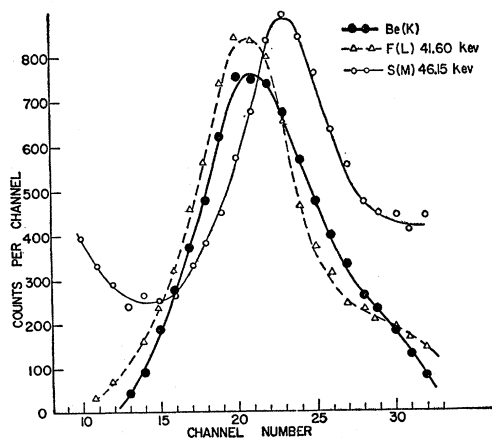


FIG. 6. Curves of the Be(K) x-rays and its calibration lines. The background has been subtracted for Be and F, but not for the S( $M$ ) line.

<sup>23</sup> D. West (private communication) and *Sixth Annual Rochester Conference on High-Energy Physics* (Interscience Publishers, Inc., New York, to be published).

background subtracted for the F( $L_\alpha$ ) and Be( $K_\alpha$ ) lines. Since the higher transitions are easily separable for L-lines ( $L_\alpha/L_\beta=1.35$ ) and M lines ( $M_\alpha/M_\beta=1.46$ ), the energy per channel was determined from the peak positions of the F( $L_\alpha$ ) and the S( $M_\alpha$ ) lines. This calibration value was then applied to the midpoints of the leading edges of the Be and F spectra to obtain the energy of the Be( $K_\alpha$ ) line. Seven complete sets of Be data were taken. The Be( $K_\alpha$ ) energy determined from these runs was  $42.09 \pm 0.10$  kev, the error being the rms value. This energy is 1.86 kev less than the calculated value and gives a shift of  $(4.2 \pm 0.25)\%$  for the  $2p \rightarrow 1s$  transition.

The Be( $K_\alpha$ ) energy measured in this way agrees excellently with that obtained from the critical absorber technique (about 42.0 kev), thereby giving us confidence in the correctness of the procedure of using the midway

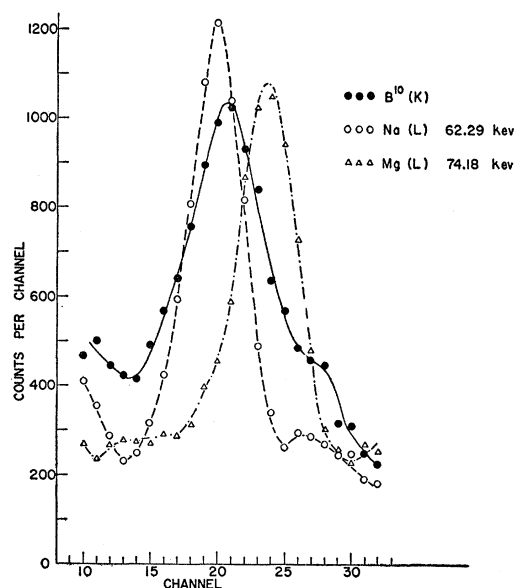


FIG. 7. Curves of the  $B^{10}(K)$  x-rays and its calibration lines. Here no background subtractions are necessary.

points of the leading edges as fiducial marks for the Be and Li determinations. This value is also in excellent agreement with that of West and Bradley<sup>24</sup> ( $42.0 \pm 0.1$  kev), who have measured the Be( $K_\alpha$ ) energy with a proportional counter.

*Boron-10 and Boron-11.*—The calibration lines were Na( $L_\alpha$ ) and Mg( $L_\alpha$ ). The backgrounds of both boron isotopes and their calibration lines were sufficiently flat and similar so that it was unnecessary to make background subtractions. No efficiency corrections were required. Figure 7 shows a typical run of  $B^{10}$  and its calibration lines. Curves of both isotopes are shown in Fig. 8. Eight complete boron series were obtained; in each case the  $B^{10} K_\alpha$  energy was higher than that of the  $B^{11}$ .

<sup>24</sup> D. West and E. F. Bradley, *Phil. Mag.* 8, 97 (1956).

The  $B^{10}$  was an enriched sample from Oak Ridge and their analysis gave  $B^{10}(84.6 \pm 0.1)\%$  and  $B^{11}(15.4 \pm 0.1)\%$ . The  $B^{11}$  target was 99% pure boron and contained the normal isotopic mixture, about 18.4%  $B^{10}$  and 81.6%  $B^{11}$ . The  $2p \rightarrow 1s$  transition energies obtained for these mixtures were  $64.96 \pm 0.15$  kev for the  $B^{10}$  sample and  $63.80 \pm 0.15$  kev for the  $B^{11}$  sample. The energies of the pure isotopes can be readily calculated from these values (assuming a Gaussian shape for the spectra). They are  $B^{10}(K_\alpha) = 65.2 \pm 0.2$  kev and  $B^{11}(K_\alpha) = 63.5 \pm 0.2$  kev. This gives an energy shift for the  $B^{10}$  of 3.54 kev, corresponding to a percent shift of  $(5.15 \pm 0.3)\%$ ,—and a shift for the  $B^{11}$  of 5.35 kev, or a percent shift of  $(7.8 \pm 0.3)\%$ . The difference in energy shift of the two isotopes is  $1.8 \pm 0.3$  kev, the percent difference being  $(2.65 \pm 0.5)\%$ . The errors quoted are the rms errors of the several series of runs.

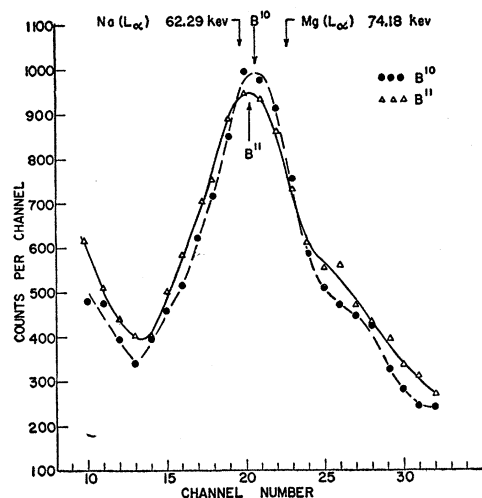


FIG. 8. Comparison of the  $K$  x-rays from the two boron isotopes,  $B^{10}$  and  $B^{11}$ . This indicates that the  $1s$  level of the  $B^{11}$  mesonic atom is shifted more than that of the  $B^{10}$ .

**Carbon-12 (98.9%).**—The calibration lines were  $Al(L_\alpha)$  and  $Si(L_\alpha)$ . Figure 9 shows typical carbon data before and after background subtractions were made. No efficiency corrections were necessary. The  $C(K_\alpha)$  energy obtained from four series of runs was  $92.6 \pm 0.4$  kev. This is 6.5 kev lower than the calculated value, corresponding to a percent shift of  $(6.5 \pm 0.4)\%$ .

**Nitrogen-14 (99.6%).**—The calibration lines were  $P(L_\alpha)$  and  $S(L_\alpha)$ . Hydrazine,  $(NH_2)_n$ , used as the  $N$  target, could only be obtained with 95% purity, the rest being  $H_2O$ . Evidence of this contamination can be seen in Fig. 10, which shows a typical nitrogen series. The oxygen line is easily resolved and leads to no difficulties. On the low-energy side is a bump due to the  $N(K_\alpha)$  escape peak and some  $C(K_\alpha)$  contamination from the third counter. These again are easily resolved. Background subtractions and efficiency corrections were made for the  $N(K)$ . The efficiency corrections turned out to be small and had no observable effect on the

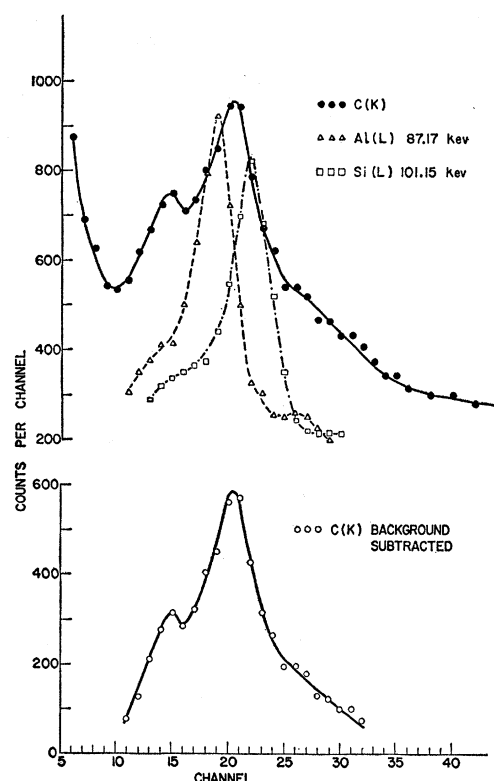


FIG. 9.  $C(K)$  curves, before and after the background subtraction, with calibration lines. The low-energy bumps are due to the escape of iodine  $K$  x-rays from the NaI detector.

$N(K_\alpha)$  energy. Seven series of runs gave a  $N(K_\alpha)$  energy of  $126.0 \pm 0.3$  kev, the error being the rms error. This gives an energy shift of the  $1s$  level of 8.8 kev, or a percent shift of the  $2p \rightarrow 1s$  transition of  $(6.55 \pm 0.2)\%$ .

**Oxygen-16 (99.8%).**—The calibration lines were the  $Cl(L_\alpha)$  and the  $Zn(M)$ . The  $Zn(M)$  peak was a secondary standard. Because of the finite resolution of the NaI detector, higher transition  $N$  lines overlapped the  $M$  peak and thus made it appear lower than the calculated value. It was therefore measured independently with  $Cl(L_\alpha)$  and  $K(L_\alpha)$  lines. The experimentally determined value was  $159.45 \pm 0.25$  kev.

Figure 11 shows a typical  $O(K)$  run with its calibration lines. Both background subtractions and efficiency corrections were made for the oxygen. The average energy of eight series of runs was  $155.2 \pm 0.8$  kev. [The quoted error is larger than the rms error of the several runs; it includes estimates of the uncertainties in the  $Zn(M)$  calibration and in background subtraction.] This corresponds to a shift of the oxygen  $1s$  level of 20.5 kev and a percent shift of the  $2p \rightarrow 1s$  transition of  $(11.7 \pm 0.5)\%$ .

**Fluorine-19 (100%).**—LiF was used as the target. The calibration lines were  $K(L_\alpha)$  and  $Ca(L_\alpha)$ . Figure 12 shows a typical run of the  $F(K)$  line before and after its background was corrected for detector inefficiency and subtracted. Four series of runs gave an energy of



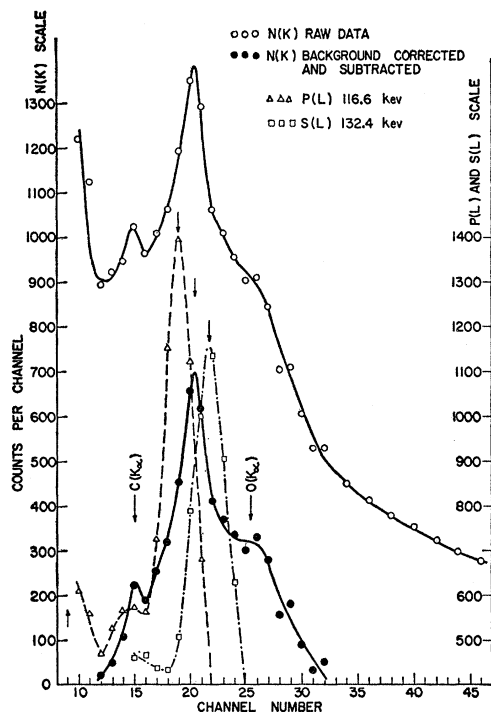


FIG. 10.  $N(K)$  curves (before and after background corrections and subtractions) with calibration lines. The low-energy peaks are due partly to the iodine escape peaks but mainly are  $C(K)$  x-rays from the third counter of the meson telescope. The high-energy bump on the  $N$  is due to higher transitions plus some  $O(K)$  line contamination. The  $N$  target was hydrazine containing about 5% water.

$196.3 \pm 1.0$  kev. The error has been increased over the rms error to include uncertainties in background subtractions and in the energy of the  $Ca(L_{\alpha})$  line. [The data were also analyzed by considering just the position of the  $K(L_{\alpha})$  peak and the zero of the p.h.s.] This gives an energy shift of 25.3 kev in the  $1s$  level or a percent shift of the  $2p \rightarrow 1s$  transition of  $11.4 \pm 0.5\%$ .

#### V. SYSTEMATIC ERRORS

The experimental errors quoted throughout are due to statistics, drifts in the electronic equipment, background subtraction, and detection efficiency corrections. Additional errors which are possibly present but more difficult to evaluate are the systematic errors. We have attempted to minimize these by consistently comparing the  $K_{\alpha}$  line under investigation with  $\pi$  lines of very nearly the same energy. This not only makes the energy measurements insensitive to the over-all linearity of the p.h.s, but it tends to cancel errors due to changes in beam strength, variations in background of the NaI detector, overloading of electronics due to abnormally large pulses, fluctuations in the duty cycle of the machine, etc. There remain two possible sources of systematic errors of which we are aware. The first is the possibility of assigning too high an energy to the  $K_{\alpha}$  line because of insufficiently resolved higher  $K$

transitions. The second is the possibility that the  $\pi$ -calibration lines themselves may have shifts due to the pion-nucleus interaction.

The effect of higher transitions is negligible in the measurements of Li and Be since for these we used the midpoints of the leading edges as fiducial marks. This effect should appear first, if at all, in the measurement of boron. The  $B(K_{\alpha})$  line has the lowest energy measured by the peak position method, and, therefore, the poorest resolution. Fortunately, as discussed in Sec. IV A, the  $B^{10}(K_{\alpha})$  line is split by the Hf  $K$  edge. From this incomplete absorption of the line by Hf and from a reasonable estimate of the line width as given by Brueckner (see Sec. VI), we can conclude that the pulse-height measurement of the  $B^{10}(K_{\alpha})$  energy cannot be wrong by more than 0.15 kev. In this case, therefore, the higher transitions do not contribute an error. It might still be argued that the fraction of higher transitions increases with greater  $Z$  and that, despite the

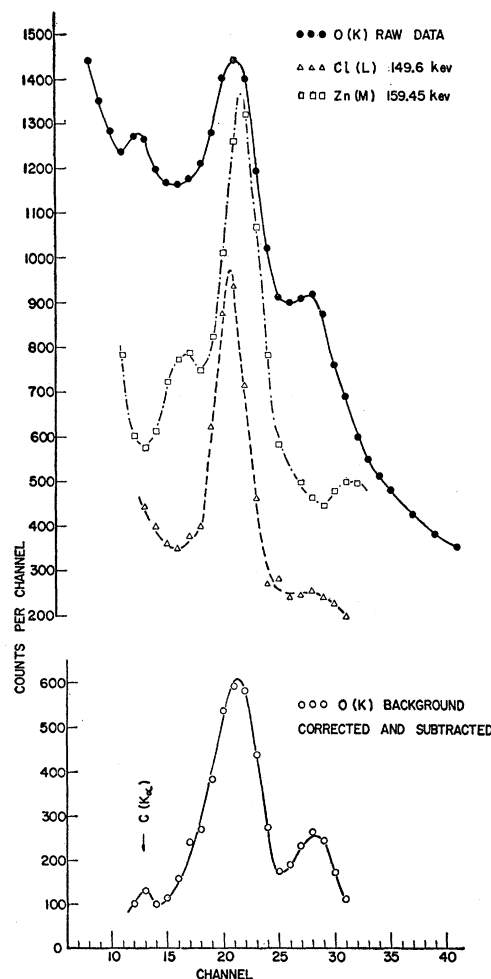


FIG. 11.  $O(K)$  curves, before and after background corrections and subtractions, with calibration lines. The low-energy  $C(K)$  peak arises from mesons stopping in the third counter of the telescope.

improved resolution at higher energies, these components might still contribute an apparent shift to higher channels. This does not appear to be the case. Our radiative yield data for both  $\pi$ -K and  $\pi$ -L lines indicate that the ratio of higher transitions stays fairly constant over the whole region of nuclear capture. Hence we are satisfied that higher transitions do not contribute any systematic error.

The second possible systematic error would be due to shifts of the  $2p$  energy levels in the calibration lines because of specific pion-nucleus interactions in this state. An upper estimate of this effect can be obtained from  $p$ -wave scattering phase shifts. Using only the  $\delta_{33}$  phase shift and assuming that the effect of the individual nucleons are additive, Wolfenstein<sup>25</sup> has derived an expression for this  $2p$  level shift.

$$\frac{\delta E}{E_{2p}} = -\frac{\mu}{\bar{\mu}} (Z\alpha)^3 \frac{\delta_{33}}{\eta^3} \left[ \frac{Z}{3} + N \right], \quad (13)$$

where  $\bar{\mu}$  is the reduced mass (with respect to a nucleon) and  $\eta$  is the meson momentum in units of  $\mu c$ . From

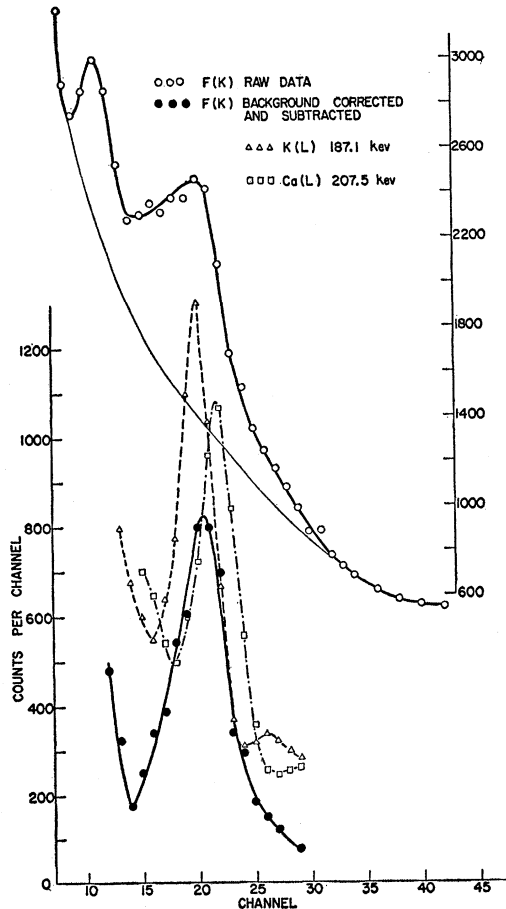


FIG. 12.  $F(K)$  curves, before and after background corrections and subtractions, with calibration lines.

<sup>25</sup> L. Wolfenstein (private communication).

TABLE III. Calculated and experimental values of the  $3d \rightarrow 2p$  transition energies.

Element	Calculated energy (kev)	Experimental energy (kev)
Si	101.15	$100.6 \pm 1.0$
Cl	149.6	$149.1 \pm 1.0$
K	187.1	$186.6 \pm 1.5$
Ca	207.5	$205.5 \pm 2.0$

Bethe and de Hoffman<sup>26</sup> one gets  $\delta_{33} \approx 0.23\eta^3$ . The percent shift of the  $3d \rightarrow 2p$  transition energy is 9/5 times the above expression. Substituting in all numerical values we get, for  $N=Z$ , the percent shift of the  $L$  lines,

$$\delta E/E_{L\alpha} = 2.5 \times 10^{-5} Z^4 \%. \quad (14)$$

This gives about a 4% shift for the  $\text{Ca}(L_\alpha)$ , the highest  $Z$  calibration line. The energy is increased because  $\delta_{33}$  is positive, implying an attractive force between the  $2p$  meson and the nucleons, and accordingly shifting the  $2p$  level downwards. There are several reasons why Eq. (13) may be an unreliable estimate: (1) although the meson is in a  $p$  state with respect to the center of mass of the nucleus it is part of the time in an  $s$  state with respect to individual nucleons. This is due to the internal momentum distribution of the nucleons. (2) The other  $p$  phase shifts,  $\delta_{31}$ ,  $\delta_{13}$ , and  $\delta_{11}$ , have been ignored in this treatment. Some may be of opposite sign and their effect may not be negligible. (3) The assumption of simple additivity is questionable; correlation effects may be important.

Because of the size of the upper estimate and the uncertainty of its validity we felt it necessary to measure the energies of some of the  $L_\alpha$  lines.  $M$  lines could not be used for calibration since higher  $N$  transitions overlap the  $M_\alpha$  and tend to reduce the measured energy.  $\mu$ -meson lines and radioactive sources were also objectionable for reasons discussed earlier in Sec. IV B. The simplest and most convenient method was to measure a relatively high- $Z$   $L_\alpha$  line with respect to a lower- $Z$   $L_\alpha$ , where the shift was expected to be negligible. For this type of measurement we must know the zero of the p.h.s. and assume linearity over a larger range than was ever assumed in the  $K_\alpha$  line measurements. It is, therefore, inherently much less accurate than the procedure used for the  $K_\alpha$  lines. The  $\text{K}(L_\alpha)$  and  $\text{Ca}(L_\alpha)$  lines were measured with respect to  $\text{S}(L_\alpha)$ ,  $\text{Cl}(L_\alpha)$  with respect to  $\text{Si}(L_\alpha)$ , and  $\text{Si}(L_\alpha)$  with respect to  $\text{Na}(L_\alpha)$ . The energies so obtained are tabulated in Table III. It should be noted that, within the error, there is agreement between the calculated and experimental values of the energies. However, the measured values appear to be systematically lower than the calculated ones. This is in the direction opposite to that predicted by Eqs. (13) and (14). This type of behavior would be expected if there were a small error in the assumed

<sup>26</sup> H. A. Bethe and F. de Hoffmann, *Mesons and Fields* (Row, Peterson and Company, Evanston, 1955), Vol. II, p. 125.

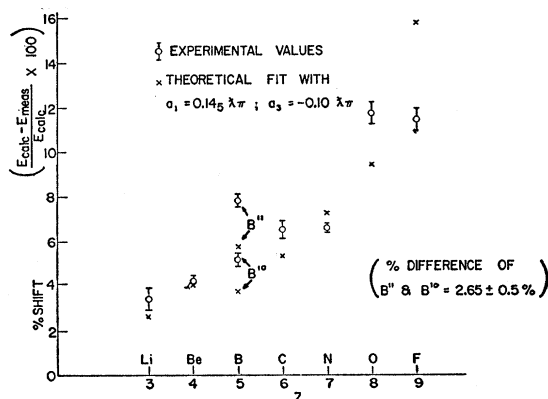


FIG. 13. Plot of the percent energy shift,  $[(E_{\text{calc}} - E_{\text{meas}})/E_{\text{calc}}] \times 100$ , of the  $2p \rightarrow 1s$  transitions vs  $Z$  of the target element. A least squares analysis of the data using the theoretical formula of Deser *et al.* gives as best values for the  $s$ -wave scattering lengths  $a_1 = 0.14\lambda_\pi$  and  $a_3 = -0.10\lambda_\pi$ . The theoretical percent shifts obtained with these scattering lengths are also shown.

zero of the pfs or if there were a slight nonlinearity over the range used—about 20 channels in these measurements.

In obtaining the errors for the  $K_\alpha$  energy measurements we have assumed, therefore, that the correct energies of the  $L_\alpha$  lines are given by the calculated values and that there is no error introduced due to uncertainties in the  $L_\alpha$  calibration lines.

## VI. COMPARISON WITH THEORY

In every case the measured  $K_\alpha$  energy is lower than its calculated electromagnetic energy, indicating a net repulsive interaction between the meson in an  $s$  state and the nucleus. The energies, energy shifts, and percent shifts are tabulated in Table II. In Fig. 13 are plotted the percent shifts,  $[(E_{\text{calc}} - E_{\text{meas}})/E_{\text{calc}}] \times 100$ . The  $\pi$ - $K_\alpha$  energies of Li, Be, and  $B^{10}$  have also been measured by West and Bradley<sup>23,24</sup> with a proportional counter. Their results are in excellent agreement with the values quoted here.

Deser *et al.*<sup>27</sup> have related the energy shift of the mesonic  $1s$  level to the meson-nucleon scattering phase shifts at zero energy. They assume that the effects of the individual nucleons are simply additive. Their expression for the fractional shift of the  $\pi$ - $K_\alpha$  line is<sup>28</sup>

$$\frac{\delta E}{E_{K_\alpha}} = -\frac{4\mu}{3\bar{\mu}} \frac{4Z}{r_B} \left[ \frac{2}{3} Z a_1 + \frac{(3N+Z)}{3} a_3 \right], \quad (15)$$

where  $\delta E$  is the energy shift in the  $1s$  level,  $r_B$  is the mesonic Bohr radius ( $1.94 \times 10^{-11}$  cm),  $a_1$  and  $a_3$  are the  $s$  scattering lengths for the isotopic spin states  $\frac{1}{2}$  and  $\frac{3}{2}$ , and  $\mu$  and  $\bar{\mu}$  are the reduced meson masses with respect to nucleus and nucleon, respectively.

<sup>27</sup> Deser, Goldberger, Bausmann, and Thirring, Phys. Rev. **96**, 774 (1954).

<sup>28</sup> Their derivation did not include the factor  $\mu/\bar{\mu}$ . This was added in accordance with the derivation given by Bethe in reference 26, p. 105.

Using our experimentally observed energy shifts for the pure isotopes, Be through F, we have made a least-squares determination of the best values of  $a_1$  and  $a_3$ . The values so obtained are  $a_1 = 0.14\lambda_\pi$  and  $a_3 = -0.10\lambda_\pi$ , where  $\lambda_\pi$  is the  $\pi$ -meson Compton wavelength. The theoretical percent shifts, plotted in Fig. 13, were calculated with these values. An independent determination of  $a_3$  can be derived from Eq. (15) using the measured energy difference between  $B^{10}$  and  $B^{11}$ . This gives  $a_3 = (-0.12 \pm 0.02)\lambda_\pi$ . These scattering lengths can be compared with Orear's<sup>29</sup> values obtained from an analysis of low-energy  $\pi$ - $p$  scattering:  $a_1 = 0.16\lambda_\pi$  and  $a_3 = -0.11\lambda_\pi$ . As can be seen, there is good agreement between the two results. This may be fortuitous. The  $1s$  level shift predicted by Deser *et al.* should vary as  $Z^2$  for  $Z=N$ . This appears to be too strong a  $Z$  dependence for the measured elements  $B^{10}$ , N, C, and O. Also the experimental fluctuations between neighboring elements do not agree very well with those predicted by Eq. (15). This disagreement with the theory may indicate that the simple assumption of additivity of the effects of individual nucleons must be modified. Brueckner has made an estimate of the effect of absorption and re-emission of the meson by pairs of nucleons and has found that it contributes a shift of about the same magnitude and sign as that due to scattering from single nucleons. Thus the total shift, as given by Brueckner, would be about twice as large as that experimentally observed—assuming reasonable values of the scattering length. (This theory is sensitive to the meson absorption rate and the internal momentum distribution of the nucleons, and a modification of these parameters would change the shift.<sup>30</sup>) In addition to the shift, the Brueckner theory gives an estimate of the line width, namely  $Z^2 E_Z / 2150$  for the half-width of the  $1s$  level. In general this is too small to be observed with our resolution. However, as described in Sec. IV A, we have been able to get a rough measure of the width of the  $B^{10}$   $K_\alpha$  line by means of critical absorbers. The half-width obtained is  $1.1 \pm 1.4$  kev. This is the same order of magnitude as that given by Brueckner,  $\sim 1.1$  kev.

## ACKNOWLEDGMENTS

We wish to thank Professor S. DeBenedetti and Mr. L. Leipuner for their cooperation in the earlier phase of this work. We are indebted to numerous members of the theoretical staff for many enlightening discussions. The invaluable assistance of Mr. J. Thompson, Mr. H. Collins, and the cyclotron crew is warmly acknowledged. We are grateful to Professor E. Creutz for his aid in procuring some of the rarer materials. We also thank Mr. S. Kellman for his assistance.

<sup>29</sup> J. Orear, Phys. Rev. **96**, 176 (1954).

<sup>30</sup> Karplus, in extending Brueckner's theory, has shown that certain choices of nucleon momentum distributions will even change the sign of the shift [*Sixth Annual Rochester Conference on High-Energy Physics* (Interscience Publishers, Inc., New York), to be published].